AIP | The Journal of Chemical Physics

CH2OH+O2 reaction rate constant measured by detecting HO2 from photofragment emission

W. C. Wang, Masako Suto, and L. C. Lee

Citation: The Journal of Chemical Physics **81**, 3122 (1984); doi: 10.1063/1.448015
View online: http://dx.doi.org/10.1063/1.448015
View Table of Contents: http://scitation.aip.org/content/aip/journal/jcp/81/7?ver=pdfcov
Published by the AIP Publishing

$CH_2OH + O_2$ reaction rate constant measured by detecting HO_2 from photofragment emission

W. C. Wang, Masako Suto, and L. C. Lee
Department of Electrical and Computer Engineering, San Diego State University, San Diego, California 92182

(Received 21 March 1984; accepted 6 June 1984)

The HO_2 radical was produced in a flow tube by the $Cl + CH_3OH \rightarrow HCl + CH_2OH$ and $CH_2OH + O_2 \rightarrow HO_2 + CH_2O$ reactions. HO_2 was detected by the $OH(A\,^2\Sigma^+ \rightarrow X\,^2\Pi)$ photofragment emission produced by photodissociative excitation of HO_2 in the vacuum ultraviolet region. Using this detection method, the rate constant for the CH_2OH and O_2 reaction was measured to be $(1.4 \pm 0.4) \times 10^{-12}$ cm^3/s.

I. INTRODUCTION

The hydroperoxyl radical HO_2 is an important intermediate in atmospheric chemistry.[1] The detection of HO_2 and the determination of its reaction rates with other atmospheric species are difficult, because its steady-state concentration in various media is always low. In the last two decades, the HO_2 radical has been extensively studied by various techniques, such as absorption,[2–6] emission,[7] laser magnetic resonance (LMR),[8] and photofragmentation.[9–11]

In our laboratory, we recently extended the photofragment technique[11] to detect HO_2 from the $OH(A\,^2\Sigma^+ \rightarrow X\,^2\Pi)$ emission. HO_2 was produced by a three-body reaction: $H + O_2 + M \rightarrow HO_2 + M$. When HO_2 was excited by the Xe resonance line at 147 nm, an emission band in the 310 ± 10 nm region was observed, which was attributed to the $OH(A\,^2\Sigma^+ \rightarrow X\,^2\Pi)$ system.

In this experiment HO_2 is produced by the following reactions[12,13]:

$$CH_3OH + Cl \rightarrow CH_2OH + HCl (k_1 = 6.3 \times 10^{-11}\ cm^3/s), \quad (1)$$

$$CH_2OH + O_2 \rightarrow HO_2 + CH_2O (k_2 = 2^{+2}_{-1} \times 10^{-12}\ cm^3/s), \quad (2)$$

where k_2 was measured by Radford[13] using LMR technique. His value is 40 times larger than that reported previously.[14]

The 1983 NASA data evaluation panel[15] indicated that the effect of wall loss of CH_2OH in Radford's measurement could have introduced a large error. A further measurement for this rate constant is desirable. CH_2OH is a possible intermediate species in the tropospheric methane oxidation cycle,[16] its reaction rate constant is thus of interest.

Here we measure k_2 by monitoring HO_2 by its $OH(A\,^2\Sigma^+ \rightarrow X\,^2\Pi)$ photofragment emission. This experiment demonstrates that the present technique is useful for the measurement of HO_2 kinetics.

II. EXPERIMENTAL

The experimental setup is shown in Fig. 1. Chlorine atoms were produced by a microwave discharge of a trace of Cl_2 in 1–3 Torr of He. The power of the microwave discharge (Opthos Instruments) was set at 30 W. Oxygen was added downstream, and methanol (CH_3OH) was fed through a movable injector of 0.63 cm o.d. with radial perforation at the end. Surrounding the injector was a flow tube which had a length of 30 cm and an inner diameter of 1.24 cm. Both the flow tube and the movable injector were coated with halocarbon wax. The linear flow velocity in the flow tube was about 1050 cm/s and the reaction time ranged from a few ms to about 20 ms, depending on the position of the injector. O_2 could enter the gas cell either near the microwave discharge or near the gas cell. The flow rate was measured by a mass flow meter (Matheson model 8160).

The excitation light source was a sealed Xe resonance lamp with a MgF_2 window. The light source intensity was monitored by a CsI photodiode (Hamamatsu R 1187). A gas mixture of 1% CH_4 in Ar at atmospheric pressure was flowed through between the Xe lamp and the gas cell in order to block the 129.5 nm line and to transmit the 147 nm line. The optical path for the gas filter is 3 cm. The photoabsorption cross sections of CH_4 are 1.8×10^{-17} cm^2 at 129.5 nm[17] and about 10^{-20} cm^2 at 147 nm.[18] The 129.5 nm line will be absorbed completely, while the 147 nm line is hardly attenuated ($< 1\%$). In fact, when the gas mixture was replaced by N_2 to let both lines through, the $OH(A \rightarrow X)$ emission intensity did not increase significantly, in contrast to our previous experiment[11] in which the OH emission intensity increased by a factor of 2–6. This result indicates that the current HO_2 production method does not produce a significant amount of H_2O. Because of its negligible concentration, H_2O will not produce a sufficient $OH(A \rightarrow X)$ emission to interfer the signal from HO_2. Therefore, the HO_2 in the cur-

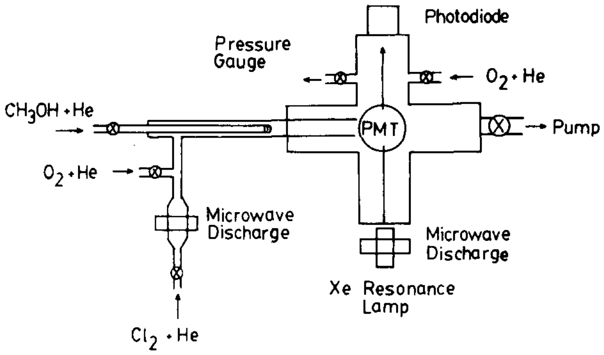

FIG. 1. Schematic diagram of the experimental setup.

0021-9606/84/193122-05$02.10

rent system can be detected by the light source of wavelength shorter than the threshold (137 nm)[19] for photodissociating H_2O into $OH(A) + H$. We have tried the Kr 123.6 nm line for detecting HO_2 in this experiment, and found the results being consistent with that of the Xe 147 nm line.

The $OH(A\,^2\Sigma^+ \rightarrow X\,^2\Pi)$ photofragment emission was detected by a cooled photomultiplier tube (PMT, EMI 9558QB) with an optical filter at 310 ± 10 nm. The PMT output signal was processed by an ORTEC pulse counting system.

The gas mixtures of 1% Cl_2 in He and 5.2% O_2 in He (supplied by Matheson) were used without purification. The O_2 concentration has been checked by measuring its absorption at 147 nm whose absorption cross section is known.[20] The methanol (supplied by Fisher, purity $\geqslant 99.9\%$) vapor was carried by He into gas cell. The concentration of methanol was determined from the ratio of the methanol vapor pressure (120 Torr at room temperature) to the pressure of carrier gas. The gas pressure was measured by a Baratron manometer (MKS Instruments).

III. RESULTS AND DISCUSSION

A. Emission from photofragment of HO_2

When HO_2 is irradiated by the Xe resonance line at 147 nm, it photodissociates,[11]

$$HO_2 + h\nu \rightarrow OH^*(A\,^2\Sigma^+) + O(^3P), \tag{3}$$

the $OH^*(A\,^2\Sigma^+)$ emits around 310 nm. The HO_2 concentration is monitored by observing the $OH(A\,^2\Sigma^+ \rightarrow X\,^2\Pi)$ emission intensity.

The emission produced from the UV photoexcitation of the reactants and products of reactions (1) and (2) was investigated. A background emission from the scattered light of the Xe lamp and from the excitation of CH_3OH (~ 30 counts/mTorr s) and Cl_2 (~ 1 count/mTorr s) by the 147 nm line was observed. The $OH(A \rightarrow X)$ emission was obtained by subtracting the background signal from the intensity observed. A chemiluminescence was observed when O_2 was added at a high flow velocity (> 1800 cm/s) and a short reaction distance. The chemiluminescence was probably caused by the reactions of O_2 with some excited species produced in the microwave discharge. This chemiluminescence is minimized by slowing down the flow velocity and increasing the reaction distance. For the loss rate measurement of CH_2OH, where the short reaction distance was required in some cases, the chemiluminescence intensity was obtained by turning off the Xe lamp and was subtracted from the total emission.

The emission intensities observed at various methanol pressures are shown in Fig. 2, where the pressures of Cl_2, O_2, and He were fixed at 13 mTorr, 20 mTorr, and 1.5 Torr, respectively. The reaction distance inside the flow tube was fixed at 9 cm, which is typical for most measurements unless specified. The emission intensity increases with increasing $[CH_3OH]$ at low pressure and reaches a plateau at pressures higher than 6 mTorr. The signal level at the high $[CH_3OH]$ corresponds to a $[HO_2]$ of about 4×10^{11} cm^{-3} in the gas cell and about 10^{13} cm^{-3} in the flow tube as compared with the $H + O_2 + M$ system.[11] Since the CH_2OH is the only expected product for the Cl and CH_3OH reaction,[12] every Cl will be converted into HO_2 if the loss is neglected. The initial [Cl] may thus be nearly equal to 10^{13} cm^{-3}. The emission was observed at a $[CH_3OH]$ as low as 0.4 mTorr as shown in Fig. 2. This result indicates that [Cl] is not higher than 0.4 mTorr, because for the case of $[Cl] > [CH_3OH]$, HO_2 will be destroyed by the excess Cl ($k = 4 \times 10^{-11}$ cm^3/s[15]) that decreases the emission signal greatly.

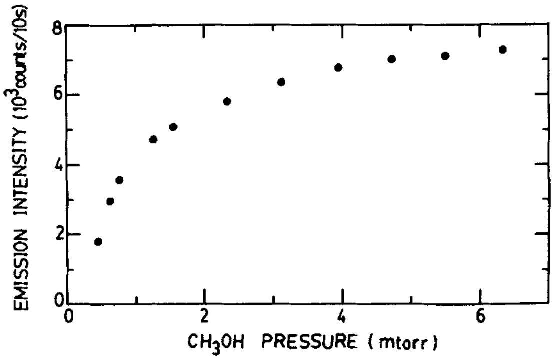

FIG. 2. The $OH(A \rightarrow X)$ emission intensity as a function of the CH_3OH pressure. The Cl_2, O_2, and He pressures are 13 mTorr, 20 mTorr, and 1.5 Torr, respectively.

The dependence of the $OH(A\,^2\Sigma^+ \rightarrow X\,^2\Pi)$ emission intensity on the Cl_2 pressure is shown in Fig. 3, where $[CH_3OH]$ is 9 mTorr, $[O_2]$ is 20 mTorr, and [He] is 1.5 Torr. The highest [Cl] or $[HO_2]$ estimated from the emission intensity is about 10^{13} cm^{-3} in the flow tube. The [Cl] increases with increasing $[Cl_2]$ at low $[Cl_2]$ and then reaches a plateau at high $[Cl_2]$.

The emission intensity vs O_2 pressure for a methanol pressure of 9.5 mTorr is shown in Fig. 4, where the Cl_2 partial pressure is 13 mTorr and the He pressure is about 1.5 Torr. The emission intensity increases with increasing O_2 partial pressure at low $[O_2]$ and reaches a plateau at high $[O_2]$. The emission intensity decreases at $[O_2] > 30$ mTorr, which is partly due to the attenuation of the 147 nm light by O_2 absorption, which will be further discussed later. The dependence of the emission intensity on $[O_2]$ is used to derive the reaction rate constant k_2 as described below.

B. Rate equations

For a first order approximation, the rate equations for the reactions (1) and (2) can be written as

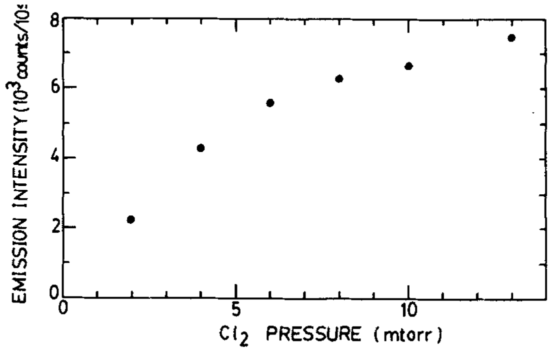

FIG. 3. The $OH(A \rightarrow X)$ emission intensity as a function of the Cl_2 pressure. The CH_3OH, O_2, and He pressures are 9 mTorr, 20 mTorr, and 1.5 Torr, respectively. The [Cl] at $[Cl_2] = 13$ mTorr is about 10^{13} cm^{-3}.

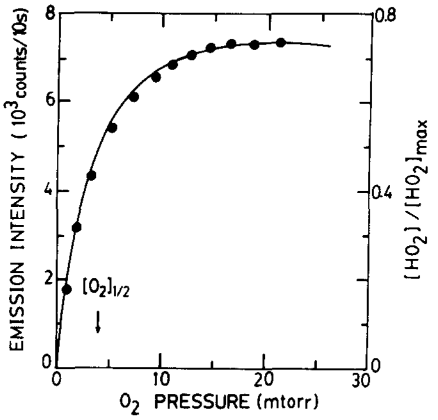

FIG. 4. The OH($A \rightarrow X$] emission intensity as a function of the O_2 pressure. The He, Cl_2, and CH_3OH are 1.5 Torr, 13 mTorr, and 9.5 mTorr, respectively. The solid line is fit by the numerical solutions of Eqs. (4a)–(4d) with $k_2 = 1.4\times10^{-12}$ cm^3/s and $k_L = 185$ s^{-1}.

$$\frac{d}{dt}[CH_3OH] = -k_1[CH_3OH][Cl], \tag{4a}$$

$$\frac{d}{dt}[Cl] = -k_1[CH_3OH][Cl], \tag{4b}$$

$$\frac{d}{dt}[CH_2OH] = k_1[CH_3OH][Cl] - k_2[O_2][CH_2OH] - k_L[CH_2OH], \tag{4c}$$

$$\frac{d}{dt}[HO_2] = k_2[CH_2OH][O_2] - k_w[HO_2], \tag{4d}$$

where k_L and k_w are the loss rates of CH_2OH and HO_2, respectively. The loss mechanism of CH_2OH could be the destruction caused by the wall or its chemical reaction with other species in the flow tube. The loss rate of HO_2 by walls is about 7 s^{-1}, as estimated from the data[11] that $[HO_2]$ decreases by a factor of 2 in a residence time of 100 ms.

When $[CH_3OH] \gg [Cl]$, as is true for most cases, $[CH_3OH]$ can be assumed constant. The $[HO_2]$ can then be obtained from solving Eqs. (4b)–(4d) analytically,

$$[HO_2] = \frac{[Cl]_0}{1+k_L/k_2[O_2]} \times \left[1 - \frac{e^{-(k_2[O_2]+k_L)t}}{1-(k_2[O_2]+k_L)/k_1[CH_3OH]}\right], \tag{5}$$

where $[Cl]_0$ is the initial value of $[Cl]$, and $k_w t \ll 1$ is assumed.

If $(k_2[O_2]+k_L)t \gg 1$, which could be satisfied by typical experimental conditions, then Eq. (5) is approximated by

$$[HO_2] \sim \frac{[Cl]_0}{1+k_L/k_2[O_2]} = \frac{[HO_2]_{max}}{1+k_L/k_2[O_2]}, \tag{6}$$

where $[HO_2]_{max}$ is measured at high $[O_2]$. The k_2 value is determined as

$$k_2 \sim k_L/[O_2]_{1/2}, \tag{7}$$

where $[O_2]_{1/2}$ is the O_2 concentration at $[HO_2]/[HO_2]_{max} = 1/2$.

The $[O_2]_{1/2}$ is obtained from the dependence of the emission intensity on the $[O_2]$ as shown in Fig. 4. Thus, k_2 will be determined if k_L is known. The k_L values measured at various Cl_2 and CH_3OH pressures are described below.

C. CH_2OH loss rate

The loss rate of CH_2OH in the flow tube k_L is measured by a slight modification of the experimental arrangement. The O_2 inlet near the microwave discharge is closed and a few mTorr of O_2 is fed through the inlet near the gas cell (see Fig. 1). Since the pumping speed is high, it is not likely that O_2 could diffuse back into the flow tube, so O_2 reacts with CH_2OH only in the gas cell. Meanwhile CH_2OH suffering its loss inside the flow tube will decay as $[CH_2OH] = [CH_2OH]_0 e^{-k_L t}$ before it reaches the gas cell, where t is the reaction time inside the flow tube. Once the CH_2OH enters the gas cell, it will react with O_2 to form HO_2. The $[CH_2OH]$ is thus equal to $[HO_2]$, which can be monitored from the OH($A\,^2\Sigma^+ \rightarrow X\,^2\Pi$) emission intensity. The k_L value can be determined from the plots of $\ln([CH_2OH]/[CH_2OH]_0)$ vs t, where the reaction time is varied by moving the position of the CH_3OH injector.

Two examples of the k_L measurements are shown in Figs. 5(a) and 5(b) where $[Cl_2] = 13$ mTorr and $[CH_3OH] = 4.7$ and 9.5 mTorr, respectively. The distance z was measured from the end of the injector to the end of the flow tube. Using the flow velocity of 1050 cm/s, k_L was determined to be 185 s^{-1} for both cases in Fig. 5.

The dependence of k_L on $[CH_3OH]$ is investigated as shown in Fig. 6. The data are taken at the Cl_2 pressure of 13 mTorr, which yields a [Cl] of about 10^{13} cm^{-3}. It should be noted that the signal level decreases with decreasing $[CH_3OH]$, so it is not practical to measure k_L at very low $[CH_3OH]$. When $[CH_3OH]$ is smaller than 1.5 mTorr, k_L increases with decreasing $[CH_3OH]$. This increase may be caused by the destruction of CH_2OH by Cl, which becomes prominent when the $[CH_3OH]$ is low.

When $[CH_3OH] > 1.5$ mTorr, k_L is approximately constant of about 185 s^{-1}. Since [Cl] is quickly consumed at high $[CH_3OH]$, it does not contribute significantly to the CH_2OH loss. Instead, the loss is mainly caused by walls. This point is further checked by measuring k_L at varied initial [Cl]. The k_L values vary less than 10% as $[Cl_2]$ varied from 2 to 13 mTorr at $[CH_3OH] \sim 5.4$ mTorr. The result clearly indicates that in the case of high $[CH_3OH]$ the de-

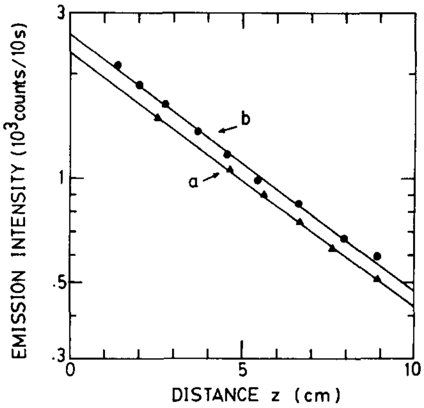

FIG. 5. The OH($A \rightarrow X$) emission intensity as a function of the CH_3OH injector position. The O_2 inlet is near the gas cell. The distance z is measured from the end of injector to the end of flow tube. The flow velocity is 1050 cm/s. The Cl_2 pressure is 13 mTorr and the pressures of CH_3OH are (a) 4.7 mTorr and (b) 9.5 mTorr.

struction of CH_2OH by Cl is negligible as compared with the wall loss, namely $k_L \sim k_{\text{wall}}$. The k_L values measured are reproducible over a long period of time.

The wall loss rate of about 185 s^{-1} measured in this experiment is larger than Radford's measurement[13] of 37 s^{-1} by a factor of 5. The loss rate depends on the experimental conditions. According to gas kinetics theory, the wall destruction in a cylinder is[21]

$$k_L = \frac{\beta \langle v \rangle}{2r}, \tag{8}$$

where β is the fraction of wall collisions that destroy CH_2OH, $\langle v \rangle$ is the mean molecular speed, and r is the radius of the flow tube. The flow tube ($r = 0.62$ cm) used in this experiment is smaller than that of Radford ($r = 1.5$ cm). This accounts for the k_L value in this experiment being larger by a factor of 2.4. The $\langle v \rangle$ values for both experiments were nearly the same, because they were both performed at room temperature. Thus, the higher k_L value in the current experiment may indicate that the current β value is larger than that of Radford's experiment by a factor of about 2.

D. $CH_2OH + O_2$ reaction rate constant

The k_L values and the O_2 dependencies of the emission intensity were measured several times. These two measurements were alternatively performed by introducing O_2 through different inlets either near the microwave discharge or near the gas cell as shown in Fig. 1.

For the determination of $[O_2]_{1/2}$ from the emission intensity as shown in Fig. 4, a correction for the attenuation of the light source intensity by O_2 needs to be made. The emission intensity is given by

$$I_e = CI_0 e^{-n\sigma l} [HO_2], \tag{9}$$

where C is a constant, n is the O_2 concentration, $\sigma = 1.4 \times 10^{-17}$ cm^2 is the absorption cross section[20] of O_2 at 147 nm, and l is the optical path length (15 cm).

The $[O_2]_{1/2}$ is about 4 mTorr as determined from Fig. 4, where the $[CH_3OH]$ of 9.5 mTorr is much larger than the $[Cl]_0$ of 10^{13} cm^{-3}, and the $[HO_2]$ is obtained from the emission intensity corrected for O_2 absorption. Substituting into Eq. (7) with $k_L = 185$ s^{-1}, the k_2 value obtained is 1.4×10^{-12} cm^3/s. The k_2 values determined for several runs are distributed within 15% of this value.

To ensure that the approximations made above are appropriate, we have solved Eqs. (4a)–(4d) numerically using $k_2 = 1.4 \times 10^{-12}$ cm^3/s and $k_L = 185$ s^{-1}, whose results are shown by the solid curve of Fig. 4. We also fit the data by the approximate solution of Eq. (5). The result is very similar to the numerical curve. This good agreement indicates that the modeling seems to be reasonable.

The secondary chemical reactions are neglected in the above modeling, which requires some justifications. The reaction rate for the Cl and CH_3OH reaction is fast, so the time period for the complete consumption of Cl is very short. Thus, for an excess of CH_3OH, the destruction of secondary species (such as CH_2OH and HO_2) by Cl is not expected to be significant. This is evident by the fact that the loss rate k_L does not depend on [Cl] at high $[CH_3OH]$ (see Fig. 6). The destruction rate of HO_2 by the secondary species is expected to be low. CH_2OH is either lost on the walls or converted to HO_2 by reaction with O_2, so it does not have enough concentration to destroy HO_2 significantly. The rate for HO_2 self-reaction is expected to be small, because the $[HO_2]$ is not larger than 10^{13} cm^{-3} in the flow tube. The rate constant[15] for the HO_2 self-reaction is 1.7×10^{-12} cm^3/s, the destruction rate is thus less than 17 s^{-1}. In a time scale of few ms, $k_w t \ll 1$, so the fraction of HO_2 destroyed by itself is small. This is supported by experimental observations that $[HO_2]$ does not decrease significantly when the reaction distances vary from 4 to 18 cm. The secondary chemical reactions are therefore negligible in the modeling.

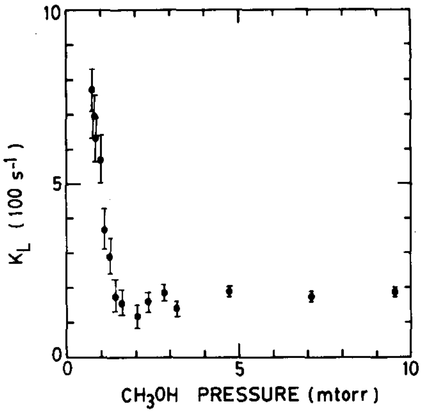

FIG. 6. The loss rate k_L of CH_2OH as a function of the CH_3OH pressure. The He and Cl_2 pressures are 1.5 Torr and 13 mTorr, respectively.

To further support the assertion that the modeling is not seriously affected by the secondary chemical reactions, we did measurements at a low $[Cl_2]$ of about 1 mTorr ($[Cl] \sim 10^{12}$ cm^{-3}). The reaction rate constant measured is consistent with the value measured at the high $[Cl_2]$ of 13 mTorr. This strengthens our conclusion that the secondary reactions are not important in the modeling.

At the lower Cl_2 concentration, HO_2 was detected with the Kr resonance lamp at 123.6 nm. This resonance line has a higher sensitivity for the HO_2 detection. However, this line can also excite H_2O to produce $OH(A \rightarrow X)$ emission, so it is only applicable when H_2O is not present. For the current HO_2 production method, the H_2O concentration is not detectable, in contrast to the $H + O_2 + M$ system that exists a high concentration of H_2O.[11]

For the case of low $[CH_3OH]$, the secondary chemical reactions become important, and modeling requires some modifications. Equation (4a) is still valid, but Eq. (4b) needs an additional term ($-k[CH_2OH][Cl]$ to account for the destruction of Cl by CH_2OH. However, this loss process may not seriously affect the Cl concentration, because CH_2OH is either quickly converted to HO_2 by O_2 or lost on the walls. Thus, Eq. (4b) may be approximately valid. The loss rate due to the Cl destruction of CH_2OH needs to be added to Eq. (4c). However, this additional loss could be made up by modifying the k_L value as shown in Fig. 6. The k_w value in Eq. (4d) should include the destruction of HO_2 by Cl. However, this additional loss rate may not be large, because [Cl] is almost consumed when HO_2 is formed. Thus,

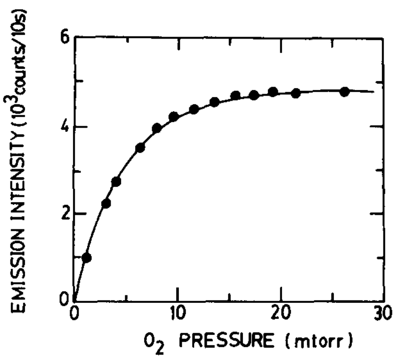

FIG. 7. The $OH(A \rightarrow X)$ emission intensity as a function of the O_2 pressure. The He, Cl_2, and CH_3OH pressures are 1.5 Torr, 13 mTorr, and 1.26 mTorr, respectively. The solid line is fit by the numerical solutions of Eqs. (4a)–(4d) with $k_2 = 1.4 \times 10^{-12}$ cm^3/s and $k_L = 280\ s^{-1}$.

$k_w t \ll 1$ still holds and k_w is again negligible in the modeling. In summary, Eqs. (4a)–(4d) can be approximately applied for the low $[CH_3OH]$ case except that k_L needs to be modified to compensate the loss rate due to the destruction of CH_2OH by Cl.

We have tested the low $[CH_3OH]$ case using the data shown in Fig. 7, where the O_2 dependence of the emission intensity was taken at $[CH_3OH] = 1.26$ mTorr, $[Cl_2] = 13$ mTorr and $[He] = 1.5$ Torr. The solid curve of Fig. 7 is the numerical solution of Eqs. (4a)–(4d) with $k_2 = 1.4 \times 10^{-12}$ cm^3/s and $k_L = 280\ s^{-1}$. The numerical solutions show a very good fit to our data. The k_L value obtained is consistent with the measured loss rate shown in Fig. 6. The k_2 value is consistent with the value obtained for the case of high $[CH_3OH]$. This good agreement further supports that our modeling is reasonable.

The experimental uncertainities are estimated to be 15% for the $[O_2]_{1/2}$, 10% for the k_L, and 10% for the flow velocity measurements. The flow rate for the He carrier gas can be measured as accurately as 2%, but since the actual flow velocity of CH_2OH is not measure, the uncertainty may be larger than this value. The CH_2OH flow velocity is assumed to be equal to the carrier gas, because the $[CH_2OH]$ is much lower than the carrier gas concentration. The overall experimental uncertainty is about 30%. The k_2 value is thus $(1.4 \pm 0.4) \times 10^{-12}$ cm^3/s. The parameters used and obtained from this experiment are summarized in Table I.

The k_2 value obtained here agrees reasonably well with Radford's value[13] of $(2^{+2}_{-1}) \times 10^{-12}$ cm^3/s, in spite of the $[CH_2OH]$ loss rates measured in these two experiments being quite different. The current experiment demonstrates that this new HO_2 detection method can be applied for measuring the reaction rate constants of HO_2 with various atmospheric species.

Table I. Values for experimental parameters.

Parameters	Value
He carrier gas	~1.5 Torr
Cl_2 partial pressure	1–13 mTorr
CH_3OH partial pressure	0.4–9.5 mTorr
Initial Cl concentration (estimated)	$(0.1\text{–}1) \times 10^{13}$ cm^{-3}
Flow velocity	1050 cm/s
Reaction time	4–20 ms
k_L for excess CH_3OH	185 s^{-1}
Reaction rate constant for $CH_2OH + O_2 \rightarrow HO_2 + CH_2O$	$(1.4 \pm 0.4) \times 10^{-12}$ cm^3/s

ACKNOWLEDGMENTS

The authors wish to thank Dr. C. J. Howard at the NOAA Environmental Research Laboratory, Dr. M. C. Lin at the Naval Research Laboratory, Dr. M. T. Leu at the Jet Propulsion Laboratory, and F. Li, Dr. E. R. Manzanares, and Dr. J. B. Nee in our laboratory for useful suggestions and discussions. This material is based on the work supported by the National Science Foundation under Grant No. ATM-8205849.

[1] P. J. Crutzen, J. Geophys. Res. **76**, 7311 (1971).
[2] T. T. Paukert and H. S. Johnston, J. Chem. Phys. **56**, 2824 (1972).
[3] C. J. Hochanadel, J. A. Ghormley, and P. J. Ogren, J. Chem. Phys. **56**, 4426 (1972).
[4] H. E. Hunziker and H. R. Wendt, J. Chem. Phys. **60**, 4622 (1974).
[5] Y. Beers and C. J. Howard, J. Chem. Phys. **63**, 4212 (1975).
[6] C. Yamada, Y. Endo, and E. Hirota, J. Chem. Phys. **78**, 4379 (1983).
[7] R. P. Tuckett, P. A. Freedman, and W. J. Jones, Mol. Phys. **37**, 379 (1979).
[8] J. T. Hougen, H. E. Radford, K. M. Evenson, and C. J. Howard, J. Mol. Spectrosc. **56**, 210 (1975).
[9] L. C. Lee, H. Helm, and J. S. Chang, Chem. Phys. Lett. **81**, 537 (1981).
[10] L. C. Lee, J. Chem. Phys. **76**, 4909 (1982).
[11] M. Suto and L. C. Lee, J. Chem. Phys. **80**, 195 (1984).
[12] J. V. Michael, D. F. Nava, W. A. Payne, and L. J. Stief, J. Chem. Phys. **70**, 3652 (1979).
[13] H. E. Radford, Chem. Phys. Lett. **71**, 195 (1980).
[14] L. I. Avramenko and R. V. Kolesnikova, Bull. Acad. Sci. USSR Div. Chem. Sci. 545 (1961).
[15] W. B. DeMore, M. J. Molina, R. T. Watson, D. M. Golden, R. F. Hampson, M. J. Kurylo, C. J. Howard, and A. R. Ravishankara, *Chemical Kinetics and Photochemical Data for Use in Stratospheric Modeling* (JPL, Pasadena, 1981), No. 81–62.
[16] J. H. Seinfeld, F. Allario, W. R. Bandeen, W. L. Chameides, D. D. Davis, E. D. Hinkley, R. W. Stewart, NASA Reference Publication No. 1062, 1981.
[17] L. C. Lee and C. C. Chiang, J. Chem. Phys. **78**, 688 (1983).
[18] K. Watanabe, M. Zelikoff, and E. C. Y. Inn, Air Force Cambridge Research Center Technical Report No. 53–23 1953.
[19] L. C. Lee, J. Chem. Phys. **72**, 4334 (1980).
[20] R. D. Hudson, Rev. Geophys. Space Phys. **9**, 305 (1971).
[21] F. Kaufman, Prog. React. Kinet. **1**, 1 (1961).